Letter

Resonant stroboscopic Rydberg dressing: Electron-motion coupling and multibody interactions

Chris Nill [1,2] Sylvain de Léséleuc [3,4] Christian Groß [5] and Igor Lesanovsky [1,6]

[1]*Institut für Theoretische Physik and Center for Integrated Quantum Science and Technology, Universität Tübingen, Auf der Morgenstelle 14, 72076 Tübingen, Germany*

[2]*Institute for Applied Physics, University of Bonn, Wegelerstraße 8, 53115 Bonn, Germany*

[3]*Institute for Molecular Science, National Institutes of Natural Sciences, 444-8585 Okazaki, Japan*

[4]*RIKEN Center for Quantum Computing (RQC), 351-0198 Wako, Japan*

[5]*Physikalisches Institut and Center for Integrated Quantum Science and Technology, Universität Tübingen, Auf der Morgenstelle 14, 72076 Tübingen, Germany*

[6]*School of Physics and Astronomy and Centre for the Mathematics and Theoretical Physics of Quantum Non-Equilibrium Systems, The University of Nottingham, Nottingham NG7 2RD, United Kingdom*

(Received 4 December 2024; accepted 14 April 2025; published 29 April 2025)

Rydberg dressing traditionally refers to a technique where interactions between cold atoms are imprinted through the far off-resonant continuous-wave excitation of high-lying Rydberg states. Dipolar interactions between these electronic states are then translated into effective interactions among ground-state atoms. Motivated by recent experiments, we investigate two dressing protocols, in which Rydberg atoms are resonantly excited in a stroboscopic fashion. The first one is nonadiabatic, meaning Rydberg states are excited by short pulses. In this case, mechanical forces among Rydberg atoms result in electron-motion coupling, which generates effective multibody interactions. In the second, adiabatic protocol, Rydberg states are excited by smoothly varying laser pulses. We show that also, in this protocol, substantial multibody interactions emerge.

DOI: 10.1103/PhysRevA.111.L041104

Introduction. Many current quantum simulation and computation platforms based on trapped ultracold atoms harness the properties of electronic Rydberg states [1–9]. These are highly excited states in which atoms are strongly polarizable and thus can interact over long distances. These interactions are typically orders of magnitude stronger than those between ground-state atoms. Additionally, the short lifetime of Rydberg states is incompatible with the timescales of ultracold quantum dynamics. Rydberg dressing is a way to overcome this problem [10,11]. In this process, the ground state of ultracold atoms is coupled to a Rydberg state via a far-detuned continuous-wave laser. This weak admixture of the Rydberg state enables sufficiently strong interactions and longer lifetimes, allowing for quantum simulations of novel phases, phase transitions, and dynamics [12–18].

Recent developments have shown that stroboscopic dressing schemes may offer advantages over the conventional Rydberg dressing approach. The underlying idea is related to earlier works which employ external periodic driving to shape dynamical processes in cold atomic gases [19–26]. In stroboscopic dressing, Rydberg states are excited periodically using laser pulses, rather than through continuous off-resonant excitation. This ensures that Rydberg states are populated only during discrete intervals, reducing overall interaction time and aligning the dynamics with the slower timescales of ultracold atoms. Pulsed excitation protocols have also been studied in Refs. [27,28] for realizing Floquet systems based on PXP models [29–31], where the Rydberg blockade prevents the simultaneous excitation of nearby Rydberg atoms.

In this work, we study theoretically resonant stroboscopic Rydberg dressing in a cold-atom tweezer array [5]. Specifically, we focus on two protocols, with the aim of creating effective spin Hamiltonians: the first involves short pulses, which break the Rydberg blockade [32–37]. In this case, the coupling between electronic excitation and the mechanical motion of atoms within their traps generates controllable spin-motion entanglement and multibody interactions that cannot be reduced to a sum of two-body terms [38,39]. The second protocol relies on slow adiabatic pulses. Here, the strength of the effectively generated multibody interactions is controlled by the detuning of the Rydberg excitation laser and the spatial separation between the atoms.

General model. We consider ultracold atoms of mass m confined in optical tweezers, as shown in Fig. 1(a), in which they perform quantized oscillatory motion, characterized by the trap frequency ω and the displacement coordinate x_j. The equilibrium distance between two neighboring atoms is a_0. The electronic degrees of freedom of each atom are modeled by two long-lived ground states ($|\downarrow\rangle$, $|\uparrow\rangle$), which form a fictitious spin, along with the Rydberg state $|r\rangle$. Rydberg atoms separated by the distance x interact with the potential $V(x)$. Considering only interactions between nearest neighbors, the Hamiltonian of this system is given by ($\hbar = 1$)

$$H_0 = \omega \sum_j a_j^\dagger a_j + V \sum_j n_j n_{j+1} + G \sum_j n_j n_{j+1}(x_j - x_{j+1}). \tag{1}$$

Here $n_j = |r\rangle\langle r|_j$ is the projector on the Rydberg state of atom j, $V = V(a_0)$ is the interaction energy between nearest-neighbor Rydberg atoms, and $G = \partial V(x)/\partial x|_{x=a_0}$ is the corresponding potential gradient [40]. The latter gives

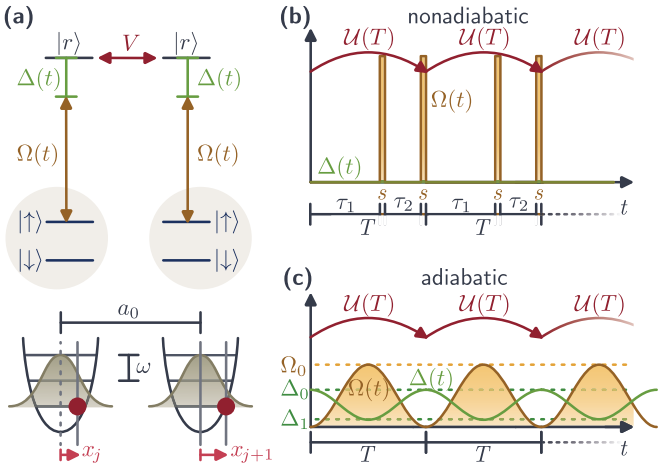

FIG. 1. Atomic levels and dressing protocols. (a) Two atoms trapped in tweezers which are modeled as one-dimensional harmonic oscillators with trapping frequency ω. Their equilibrium separation is a_0, and the displacement from their individual equilibrium positions is given by x_j and x_{j+1}, respectively. Each atom is modeled by two long-lived ground states ($|\uparrow\rangle$, $|\downarrow\rangle$) and a Rydberg state $|r\rangle$. Neighboring atoms in the state $|r\rangle$ interact with the strength V. A globally applied laser couples $|\uparrow\rangle$ and $|r\rangle$ with the time-dependent Rabi frequency $\Omega(t)$ and the detuning $\Delta(t)$. (b) The dressing protocols consist of periodic sequences of pulses of length T. In the nonadiabatic dressing protocol, two short π pulses of duration s are applied, which break the Rydberg blockade [see Eq. (3)]. In between the two pulses, interacting Rydberg states are excited, which generates effective interactions among atoms in the state $|\uparrow\rangle$. (c) In the adiabatic dressing protocol, the Rabi frequency $\Omega(t)$ and the detuning $\Delta(t)$ are varied smoothly [see Eqs. (9) and (10)]. Rydberg states are excited during the pulses, but deexcited at the end. Dynamical phases accumulated during this process translate into effective interactions among atoms in the state $|\uparrow\rangle$.

rise to a coupling between electronic and motional degrees of freedom, which are represented through raising and lowering operators: $x_j = x_0(a_j + a_j^\dagger)$, with the harmonic oscillator length $x_0 = \sqrt{1/(2m\omega)}$.

The idea of Rydberg dressing is to generate effective interactions among atoms in the state $|\uparrow\rangle$ (see Fig. 1) by virtually or temporarily coupling this state to the Rydberg level $|r\rangle$. This coupling is achieved by a laser with the time-dependent detuning (with respect to the $|\uparrow\rangle$-$|r\rangle$ transition) $\Delta(t)$ and the Rabi frequency $\Omega(t)$. This laser coupling is described by the Hamiltonian [41]

$$H_{\mathrm{L}}(t) = \Omega(t)\sum_j (|\uparrow\rangle\langle\uparrow|r_j e^{-i\kappa x_j} + \mathrm{H.c.}) + \Delta(t)\sum_j n_j, \quad (2)$$

where κ is the projection of the laser wave vector onto the axis connecting neighboring atoms (we assume here that the atoms are positioned on a one-dimensional (1D) chain in the x direction). In this work, we consider stroboscopic dressing pulses, i.e., the laser parameters $\Delta(t)$ and $\Omega(t)$, are periodic functions with period T, as shown in Fig. 1. Our goal is to derive expressions for the time-evolution operator $\mathcal{U}(T)$ that propagates the system from the stroboscopic time nT to $(n+1)T$. Rydberg states will only be excited during the dressing pulses, but (ideally) Rydberg excitations are present neither in the initial state nor in the states which the system assumes at the end of each pulse. Therefore, the time-evolution operator $U(T)$ only operates in the $|\uparrow\rangle$-$|\downarrow\rangle$ manifold and is generated by an effective spin Hamiltonian, which we construct in the following for two different dressing protocols.

Nonadiabatic dressing protocol. This protocol, which is shown in Fig. 1(b), consists of two short resonant π pulses applied during a dressing cycle. Each pulse has duration s; one is applied at time τ_1 and the other at time $T - s$. Mathematically, this sequence is modeled by choosing the parameters of the laser Hamiltonian (2) as $\Delta(t) = 0$ and

$$\Omega(t) = \frac{\pi}{2s}\big[\Pi_{\tau_1,\tau_1+s}(t) + \Pi_{T-s,T}(t)\big], \quad (3)$$

where $\Pi_{a,b}(t) = \Theta(t-a) - \Theta(t-b)$ and Θ is the Heaviside step function. One dressing cycle can be decomposed as follows. The system starts at $t = 0$ in a spin state, $|\psi_0\rangle$, where no Rydberg excitations are present. During the time interval $0 \leqslant t \leqslant \tau_1$, the system evolves under the Hamiltonian H_0, Eq. (1), since the laser Hamiltonian H_L is 0. No Rydberg excitations are created, since H_0 conserves the total excitation number. The first π pulse excites all $|\uparrow\rangle$ states to the Rydberg state $|r\rangle$. This assumes that the pulse is sufficiently strong in order to overcome the interaction among Rydberg atoms; i.e., it needs to break the Rydberg blockade, which is possible when $V \ll \pi/(2s)$. Note that this process may also lead to oscillatory excitations due to momentum transfer from the laser to the atoms. In the following time interval of length τ_2, nearest-neighbor atoms in the Rydberg state interact, and further coupling between the electronic and motional degrees of freedom occurs. The dressing cycle concludes with a second π pulse, applied during the time interval $T - s \leqslant t \leqslant T$, that deexcites the Rydberg states.

The time-evolution operator which propagates the system over a dressing cycle of duration T can be expressed as a product of unitary operators. For a general pulse duration s, this is

$$\mathcal{U}(T, s) = e^{-is(H_{\mathrm{L}}+H_0)}e^{-iH_0\tau_2}e^{-is(H_{\mathrm{L}}+H_0)}e^{-iH_0\tau_1}. \quad (4)$$

In the limit of short π pulses, i.e., for pulses in which $s \ll t_0$ is smaller than any timescale t_0 in the free evolution due to H_0, the time-evolution operator can be calculated analytically [42], yielding

$$\mathcal{U}(T) = \prod_j e^{-iTH_{j,\mathrm{eff}}}\mathcal{D}(\mathcal{J}_j)e^{-iT\omega a_j^\dagger a_j}. \quad (5)$$

We note that recent experiments [39,43] have demonstrated that this condition can indeed be met. In the following, we analyze the terms of $\mathcal{U}(T)$ step by step. We begin with the last term, $e^{-iT\omega a_j^\dagger a_j}$, which is the simplest one and describes the free oscillatory motion of the atoms in their traps over the length T of a dressing cycle. The first term of $\mathcal{U}(T)$ is the evolution under the effective spin Hamiltonian $H_{j,\mathrm{eff}}$, which describes the time evolution of the spin at site j during a dressing cycle as

$$H_{j,\mathrm{eff}} = \frac{\tau_2 V}{T}\mathcal{P}_j\mathcal{P}_{j+1} + \frac{\tau_2}{T}\frac{\mathcal{G}_j^2}{\omega}[\mathrm{sinc}(\omega\tau_2) - 1] + \frac{\eta^2\sin(\omega\tau_2)}{T}\mathcal{P}_j + \frac{\pi}{T}\mathcal{P}_j. \quad (6)$$

Here, the first term is the "conventional" dressing potential, i.e., the interaction V among Rydberg atoms in Hamiltonian (6), is mapped onto atoms in the $|\uparrow\rangle$ state but with the weaker effective strength $V_{\text{eff}} = \tau_2 V/T$ and the projector $\mathcal{P}_j = |\uparrow\rangle\langle\uparrow|_j$. The factor of τ_2/T is the proportion of the time during which the system is in the Rydberg state during a dressing cycle. Further terms emerge in the effective spin Hamiltonian, with the next one being an interaction that is mediated by the oscillation of the atoms in their tweezer traps. It depends on the gradient G and the oscillator length x_0 through the operator

$$\mathcal{G}_j = \begin{cases} Gx_0\mathcal{P}_j\mathcal{P}_{j+1}, & \text{for } N = 2, \\ Gx_0\mathcal{P}_j(\mathcal{P}_{j+1} - \mathcal{P}_{j-1}), & \text{for } N > 2. \end{cases} \tag{7}$$

For two atoms, this contribution, which is generated by the coupling between electronic and motional degrees of freedom, merely modifies the interaction strength between atoms in the $|\uparrow\rangle$ state. For more than two atoms, however, it results in a multibody interaction [44,45]. This can be understood as follows: when an atom j is surrounded by two or no atoms in the $|\uparrow\rangle$ state, the net mechanical force acting on it when excited to the $|\uparrow\rangle$ state is 0. Hence, $\mathcal{G}_j = 0$. For other configurations, $\mathcal{G}_j$ assumes a nonzero value. Distinguishing these cases necessitates an operator which acts on site j as well as on the two neighboring sites, hence generating a three-body interaction. The term $\eta^2 \sin(\omega\tau_2)\mathcal{P}_j/T$ in the effective Hamiltonian accounts for the momentum transfer during laser excitation. It is quantified by the Lamb-Dicke parameter $\eta = \kappa x_0$ [46–48]. The last term, $\frac{\pi}{T}\mathcal{P}_j$, arises due to the application of two π pulses during the dressing cycle, which leads to a phase shift of π for all atoms in the state $|\uparrow\rangle$.

Let us now return to the middle term of the unitary evolution operator (5). It depends on the displacement operator $\mathcal{D}(\mathcal{J}_j) = \exp \mathcal{J}_j a_j^\dagger - \mathcal{J}_j^\dagger a_j$, with argument $\mathcal{J}_j = (\frac{\mathcal{G}_j}{\omega} + i\eta\mathcal{P}_j)(e^{-i\omega\tau_2} - 1)$. It displaces atom j in position (momentum) space by the real (imaginary) part of $\mathcal{J}_j$, which is an operator that acts on the spin degrees of freedom [49]. This term therefore results in spin-motion coupling. The amount of the displacement further depends on the oscillation phase $\omega\tau_2$, which can be utilized to control the spin-motion coupling. If the oscillation phase is 0 or a multiple of 2π, $\mathcal{J}_j$ vanishes and spin and motional degrees of freedom decouple.

For a dressing cycle with such decoupled spin and motion, the time-evolution operator separates into an operator acting on the spins,

$$\mathcal{U}_{\text{spin}}(T) = \prod_j e^{-iTH_{j,\text{eff}}}, \tag{8}$$

and one acting on the harmonic oscillatory motion of the atoms, $\mathcal{U}_{\text{osc}} = \prod_j e^{-iT\omega a_j^\dagger a_j}$. However, multibody interactions still remain in the effective spin Hamiltonian due to its dependence on $\mathcal{G}_j^2$.

To illustrate the effect of the spin-motion coupling, we consider in Fig. 2 a system of two atoms which are initialized in the motional ground state $|0\rangle_j$. As the initial state, we choose $|\psi_0\rangle = \bigotimes_{j=1}^{N=2}[\frac{1}{\sqrt{2}}(|\uparrow\rangle_j + |\downarrow\rangle_j) \otimes |0\rangle_j]$, which is not an eigenstate of the effective spin Hamiltonian and thus leads to nontrivial dynamics. In the figure, we study the dynamics

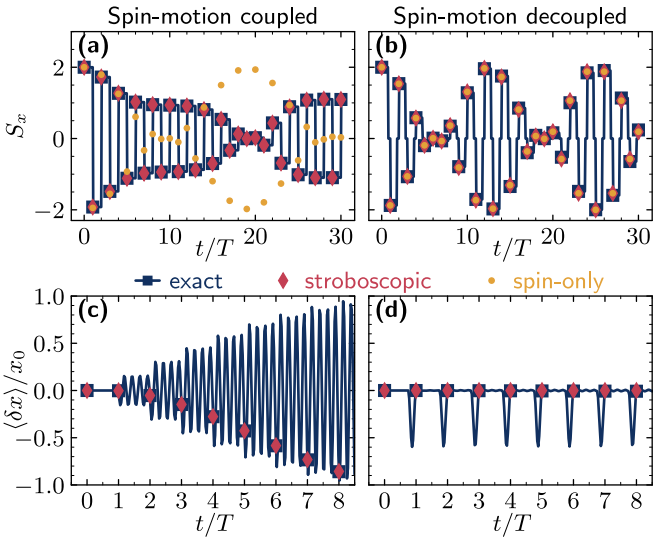

FIG. 2. Nonadiabatic dressing protocol. (a) Evolution of the expectation value of the total spin component S_x for two atoms (see text). Choosing $\omega\tau_2 = 0.01\pi$, the oscillatory motion is coupled to the spin dynamics. This leads to entanglement between the two degrees of freedom, causing spin decoherence (see Supplemental Material [42]). Numerically exact results calculated by $\mathcal{U}(T, s)$, Eq. (4), are shown as blue squares, and the stroboscopic evolution under the unitary $\mathcal{U}(T)$, Eq. (5), is shown as red diamonds. For comparison, we show the evolution of S_x in the absence of this spin-motion coupling calculated by Eq. (8) with yellow dots. The initial state $|\psi_0\rangle$ is defined in the main text. (b) When choosing $\omega\tau_2 = 2\pi$, spin and motion decouple. (c) Dynamics of the average interatomic distance $\langle\delta x\rangle$ (see text). For $\omega\tau_2 = 0.01\pi$, spin-motion coupling results in oscillations of the interatomic distance after a dressing cycle. (d) When choosing $\omega\tau_2 = 2\pi$, the motional degrees of freedom return to their initial state after each cycle. In all simulations the harmonic oscillator basis is truncated to contain a maximum of five excitations, and the parameters values are $T = 8.1\pi/\omega$, $V = 10.1\omega$, $\eta = 0.6$, and $s = \pi/(2 \times 10^4\omega)$. For panels (a) and (c), we use $Gx_0 = 5\omega$, and for panels (b) and (d), we set $Gx_0 = 0.3\omega$. Note that, in experiment, the values for V and G can, in fact, be tuned independently using microwave dressing of Rydberg states [50–53].

of two observables of the system: the expectation value of the x component of the total spin, $S_x = \sum_{j=1}^{N=2}\langle|\uparrow\rangle\langle\uparrow|\downarrow\rangle_j + |\downarrow\rangle\langle\downarrow|\uparrow\rangle_j\rangle$, and the expectation value of the distance $\langle\delta x\rangle/x_0 = \langle x_2 - x_1\rangle/x_0$ between the atoms. The time evolution of the observables is calculated numerically exactly through $\mathcal{U}(T, s)$ for finite π pulse length s, Eq. (4), and compared to the time evolution operator $\mathcal{U}(T)$ in the short-pulse limit $s \ll t_0$, Eq. (5). For $\omega\tau_2 = 2\pi$, both degrees of freedom perform a separable evolution, where the spins perform oscillations in the observable S_x. Conversely, spins and motion couple when $\omega\tau_2 = 0.1\pi$, which results in a nontrivial spin-dynamic of S_x compared to the spin-only dynamics. This is shown in Figs. 2(a) and 2(b), where we display the behavior of the spin observable S_x as a function of time for both cases. Spin-motion coupling also affects the evolution of the distance $\langle\delta x\rangle$ between the atoms: With spin-motion coupling, the distance varies strongly at each stroboscopic time step nT, while it remains constant in the decoupled case [see Figs. 2(c) and 2(d)]. To approximately decouple spin and motion, one can

scale the time interval τ_2 between the pulses to yield $\omega\tau_2 \ll 1$ (while adjusting V such that $V_{\text{eff}} = V\tau_2/T$ remains on the order of unity). Dressing with such ultrastrong laser pulses has been experimentally demonstrated in Refs. [39,43]. We discuss this special case in the Supplemental Material [42]. There, we also illustrate how a spin-motion echo sequence can decouple spin and motional dynamics.

Adiabatic dressing protocol. This dressing protocol employs slowly changing laser parameters rather than short pulses. It is sketched in Fig. 1(c). The time evolution during a dressing cycle of length T is assumed to be adiabatic, in the sense that the spin state at its beginning and its end is the same. Moreover, the state shall be smoothly connected to the instantaneous eigenstates during the adiabatic pulse, which contain components of Rydberg states. This necessity to be slow, i.e., to avoid nonadiabatic transitions, is in conflict with the finite lifetimes of Rydberg states. Hence, an appropriate parameter regime needs to be identified that ensures pulses which are much shorter than the Rydberg atom's lifetime. This is indeed possible, as shown in the Supplemental Material [42]. There, we additionally show that, for strongly trapped atoms, one can neglect the coupling between the electronic degrees of freedom and the oscillatory motion [54–62]. For simplicity, and to make the calculations tractable, we disregard spin-motion coupling in the following, setting the potential gradient G and the Lamb-Dicke parameter η to 0.

In the adiabatic dressing protocol, the Rabi frequency and the detuning are smoothly varied according to Fig. 3(a) as

$$\Omega(t) = \Omega_0 \sin^2(\pi t/T), \tag{9}$$

$$\Delta(t) = \Delta_0 - (\Delta_0 - \Delta_1)\sin^2(\pi t/T). \tag{10}$$

The dynamical phase that is accumulated during this pulse differs for each spin configuration and yields an effective Hamiltonian in the spin space which in general contains multibody interactions. As an example, we consider a system with $N = 3$ atoms positioned in an equilateral triangle whose sides have the length a_0. The effective spin Hamiltonian can generally be written in terms of the projectors $\mathcal{P}_j = |{\uparrow}\rangle\langle{\uparrow}|_j$:

$$H_{\text{eff}} = \mathcal{V}_3\mathcal{P}_1\mathcal{P}_2\mathcal{P}_3 + \mathcal{V}_2\sum_{i\neq j}\mathcal{P}_i\mathcal{P}_j + \mathcal{V}_1\sum_i \mathcal{P}_i + \mathcal{V}_0, \tag{11}$$

where $\mathcal{V}_k$ describes the effective k-body interaction strength. The evolution under this effective spin Hamiltonian over a time T then generates the dynamical phase $\varphi_{\mathcal{C}}$ of the spin configuration $\mathcal{C} \in \{{\downarrow\downarrow\downarrow}, {\downarrow\downarrow\uparrow}, \ldots, {\uparrow\uparrow\uparrow}\}$:

$$e^{-iH_{\text{eff}}T} = \sum_{\mathcal{C}} e^{-i\varphi_{\mathcal{C}}}|\mathcal{C}\rangle\langle\mathcal{C}|. \tag{12}$$

Comparing coefficients, we can now link the k-body interaction strength to the dynamical phases. Due to the symmetry of the system, the phases $\varphi_{\mathcal{C}}$ depend only on $|{\uparrow}\rangle$ spins that are contained in configuration $\mathcal{C}$. We thus use a shorthand notation, φ_α, where the subscript α refers to the number of atoms in the $|{\uparrow}\rangle$ state; i.e., we have $\varphi_{\downarrow\downarrow\downarrow} = \varphi_0$, $\varphi_{\uparrow\downarrow\downarrow} = \varphi_{\downarrow\uparrow\downarrow} = \varphi_{\downarrow\downarrow\uparrow} = \varphi_\uparrow$, etc. With this, we obtain

$$\begin{aligned} \mathcal{V}_0 T &= \varphi_0, & \mathcal{V}_1 T &= \varphi_\uparrow - \varphi_0, \\ \mathcal{V}_2 T &= \varphi_{\uparrow\uparrow} - 2\varphi_\uparrow + \varphi_0, & \mathcal{V}_3 T &= \varphi_{\uparrow\uparrow\uparrow} - 3\varphi_{\uparrow\uparrow} + 3\varphi_\uparrow - \varphi_0. \end{aligned} \tag{13}$$

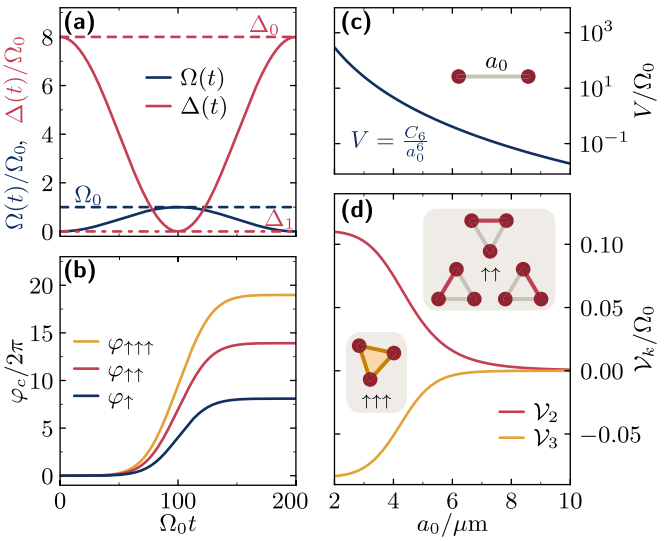

FIG. 3. Adiabatic dressing protocol. (a) Time-dependent Rabi frequency $\Omega(t)$ and detuning $\Delta(t)$ for a dressing cycle with duration $T = 200/\Omega_0$, where $\Delta_0 = 8\Omega_0$ and $\Delta_1 = 0$. (b) Accumulated dynamical phase $\varphi_{\mathcal{C}}$ in a system of three atoms placed on an equilateral triangle. Here, the initial configurations $\mathcal{C}$ need to be distinguished only by their number of atoms in the $|{\uparrow}\rangle$ state. The interaction strength is $V = 4\Omega_0$. (c) Bare van der Waals interaction between Rydberg atoms as a function of the interatomic distance a_0. We use the dispersion coefficient $C_6 = 119$ GHZ μm^6 of state $61S_{1/2}$ of potassium with the Rabi frequency $\Omega_0 = 2\pi \times 1$ MHz. (d) Effective two- and three-body interaction strength, $\mathcal{V}_2$ and $\mathcal{V}_3$, for varying interatomic distance a_0. The calculation is based on the bare van der Waals interaction shown in panel (c). The closer the interatomic distance, the higher is the relative contribution of the three-body interaction $\mathcal{V}_3$.

In the following, we construct the effective spin Hamiltonian (11) for an exemplary case and show that indeed rather generically three-body interactions emerge.

Using numerical integration [63], we solve for each initial state from $\mathcal{C}$ the time-dependent Schrödinger equation with the Hamiltonian $H(t) = H_0 + H_{\text{L}}(t)$ [Eqs. (1) and (2)] and the adiabatic pulse [Eqs. (9) and (10)]. We then extract the adiabatically accumulated dynamical phase $\varphi_{\mathcal{C}}$ as a function of the laser parameters and the interaction strength V. An example is shown in Fig. 3(b). From these phases, we can then calculate the interaction coefficients $\mathcal{V}_k$ using the above-described procedure. We assume here that the bare interaction between atoms in Rydberg states is given by a van der Waals interaction of the form $V = C_6/a_0^6$ [see Fig. 3(c)], where C_6 is the dispersion coefficient [64]. Based on this, we calculate the effective k-body interaction strength as a function of the interatomic distance a_0, which is shown in Fig. 3(d). This results in two- and three-body potentials, which have a characteristic flat-top form [65]. The larger the interparticle separation, i.e., the smaller the bare interaction V, the more dominant becomes the two-body interaction. A detailed analysis of the ratio $\mathcal{V}_3/\mathcal{V}_2$ is outlined in the Supplemental Material [42].

Conclusions and outlook. We discussed the theory underlying two stroboscopic Rydberg dressing protocols for generating effective spin Hamiltonians. The nonadiabatic protocol relies on the application of fast resonant laser pulses

which break the Rydberg blockade. This results in state-dependent mechanical forces causing a coupling between motional and electronic degrees of freedom. As a consequence, effective multibody spin interactions are generated, but also spin decoherence emerges which can be mitigated by an appropriate timing of the laser pulses. The adiabatic protocol, on the other hand, is implemented by smoothly varying laser pulses. During the adiabatic evolution, the system probes interacting configurations of Rydberg atoms, which generate spin-dependent dynamical phases resulting in effective k-body spin interactions. For a system of three atoms, we analyzed two-body and three-body interactions and their dependence on the interparticle distance.

There are a number of avenues for interesting future work. The considerations of this Letter are based on simple 1D and 2D systems, and the effect of different lattice geometries and multidimensional oscillatory excitations certainly merits further exploration. Additionally, quantum optimal control techniques may allow engineering stroboscopic dressing protocols that reduce spin-motion coupling or enhance adiabaticity while minimizing spin decoherence. In particular, it would be interesting to explore whether two-body interactions could be completely removed, leading to many-body Hamiltonians that feature solely multibody interactions.

Acknowledgments. We thank W. Martins, A. Cabot, and J. Wilkinson for fruitful discussions. We acknowledge funding from the Deutsche Forschungsgemeinschaft within Project No. GR4741/4 and the research units FOR5413 (Grant No. 465199066) and FOR5522 (Grant No. 499180199). This work builds on ideas which were developed when applying to the JST-DFG 2024: Japanese-German Joint Call for Proposals on "Quantum Technologies" (Japan-JST-DFG-ASPIRE 2024) and for which funding will be received under DFG Grant No. 554561799. We also acknowledge funding from the Horizon Europe programme HORIZON-CL4-2022-QUANTUM-02-SGA via Project No. 101113690 (PASQuanS2.1) and via the Horizon-MSCA-Doctoral Network QLUSTER (HORIZON-MSCA-2021-DN-01-GA101072964), the Alfried Krupp von Bohlen and Halbach Foundation, and the state of Baden-Württemberg through bwHPC Grant No. INST 40/575-1 FUGG (JUSTUS 2 cluster). S.d.L. acknowledges funding from the MEXT Quantum Leap Flagship Program (MEXT Q-LEAP) under Grant No. JPMXS0118069021 and JST Moonshot R&D Program Grant No. JPMJMS2269. C.G. and S.d.L. acknowledge funding from the NINS-DAAD exchange program (Quantum Simulation/Computation: From Rydberg Dressing to Ultrafast Interaction).

[1] T. F. Gallagher, *Rydberg Atoms*, Cambridge Monographs on Atomic, Molecular and Chemical Physics (Cambridge University, Cambridge, England, 1994).

[2] M. Saffman, T. G. Walker, and K. Mølmer, Quantum information with Rydberg atoms, Rev. Mod. Phys. **82**, 2313 (2010).

[3] H. Bernien, S. Schwartz, A. Keesling, H. Levine, A. Omran, H. Pichler, S. Choi, A. S. Zibrov, M. Endres, M. Greiner, V. Vuletić, and M. D. Lukin, Probing many-body dynamics on a 51-atom quantum simulator, Nature (London) **551**, 579 (2017).

[4] M. Morgado and S. Whitlock, Quantum simulation and computing with Rydberg-interacting qubits, AVS Quantum Sci. **3**, 023501 (2021).

[5] A. Browaeys and T. Lahaye, Many-body physics with individually controlled Rydberg atoms, Nat. Phys. **16**, 132 (2020).

[6] W. Lee, M. Kim, H. Jo, Y. Song, and J. Ahn, Coherent and dissipative dynamics of entangled few-body systems of Rydberg atoms, Phys. Rev. A **99**, 043404 (2019).

[7] H. Levine, A. Keesling, G. Semeghini, A. Omran, T. T. Wang, S. Ebadi, H. Bernien, M. Greiner, V. Vuletić, H. Pichler, and M. D. Lukin, Parallel implementation of high-fidelity multiqubit gates with neutral atoms, Phys. Rev. Lett. **123**, 170503 (2019).

[8] M. Magoni, R. Joshi, and I. Lesanovsky, Molecular dynamics in Rydberg tweezer arrays: Spin-phonon entanglement and Jahn-Teller effect, Phys. Rev. Lett. **131**, 093002 (2023).

[9] J. T. Wilson, S. Saskin, Y. Meng, S. Ma, R. Dilip, A. P. Burgers, and J. D. Thompson, Trapping alkaline earth Rydberg atoms optical tweezer arrays, Phys. Rev. Lett. **128**, 033201 (2022).

[10] Y.-Y. Jau, A. M. Hankin, T. Keating, I. H. Deutsch, and G. W. Biedermann, Entangling atomic spins with a Rydberg-dressed spin-flip blockade, Nat. Phys. **12**, 71 (2016).

[11] J. Zeiher, R. van Bijnen, P. Schauß, S. Hild, J.-y. Choi, T. Pohl, I. Bloch, and C. Gross, Many-body interferometry of a Rydberg-dressed spin lattice, Nat. Phys. **12**, 1095 (2016).

[12] P. Fromholz, M. Tsitsishvili, M. Votto, M. Dalmonte, A. Nersesyan, and T. Chanda, Phase diagram of Rydberg-dressed atoms on two-leg triangular ladders, Phys. Rev. B **106**, 155411 (2022).

[13] R. M. W. van Bijnen and T. Pohl, Quantum magnetism and topological ordering via Rydberg dressing near Förster resonances, Phys. Rev. Lett. **114**, 243002 (2015).

[14] J. Zeiher, J.-y. Choi, A. Rubio-Abadal, T. Pohl, R. van Bijnen, I. Bloch, and C. Gross, Coherent many-body spin dynamics in a long-range interacting Ising chain, Phys. Rev. X **7**, 041063 (2017).

[15] A. Geißler, I. Vasić, and W. Hofstetter, Condensation versus long-range interaction: Competing quantum phases in bosonic optical lattice systems at near-resonant Rydberg dressing, Phys. Rev. A **95**, 063608 (2017).

[16] R. Khasseh, S. H. Abedinpour, and B. Tanatar, Phase diagram and dynamics of Rydberg-dressed fermions in two dimensions, Phys. Rev. A **96**, 053611 (2017).

[17] E. Guardado-Sanchez, P. T. Brown, D. Mitra, T. Devakul, D. A. Huse, P. Schauß, and W. S. Bakr, Probing the quench dynamics of antiferromagnetic correlations in a 2D quantum Ising spin system, Phys. Rev. X **8**, 021069 (2018).

[18] P. Weckesser, K. Srakaew, T. Blatz, D. Wei, D. Adler, S. Agrawal, A. Bohrdt, I. Bloch, and J. Zeiher, Realization of a Rydberg-dressed extended Bose Hubbard model, arXiv:2405.20128.

[19] P. J. Bardroff, I. Bialynicki-Birula, D. S. Krähmer, G. Kurizki, E. Mayr, P. Stifter, and W. P. Schleich, Dynamical localization: Classical vs quantum oscillations in momentum spread of cold atoms, Phys. Rev. Lett. **74**, 3959 (1995).

[20] R. Blümel, *Chaos in Atomic Physics*, Cambridge Monographs on Atomic, Molecular, and Chemical Physics, Vol. 10 (Cambridge University, Cambridge, England, 1997).

[21] M. Frasca, Strong laser–atom interaction as a quantum kicked dynamics, Phys. Lett. A **290**, 277 (2001).

[22] F. Haake, *Quantum Signatures of Chaos*, Springer Series in Synergetics, Vol. 54 (Springer, Berlin, 2010).

[23] F. L. Moore, J. C. Robinson, C. Bharucha, P. E. Williams, and M. G. Raizen, Observation of dynamical localization in atomic momentum transfer: A new testing ground for quantum chaos, Phys. Rev. Lett. **73**, 2974 (1994).

[24] F. L. Moore, J. C. Robinson, C. F. Bharucha, B. Sundaram, and M. G. Raizen, Atom optics realization of the quantum δ-kicked rotor, Phys. Rev. Lett. **75**, 4598 (1995).

[25] J. C. Robinson, C. F. Bharucha, K. W. Madison, F. L. Moore, B. Sundaram, S. R. Wilkinson, and M. G. Raizen, Can a single-pulse standing wave induce chaos in atomic motion? Phys. Rev. Lett. **76**, 3304 (1996).

[26] J. A. Yeazell, M. Mallalieu, and C. R. Stroud, Observation of the collapse and revival of a Rydberg electronic wave packet, Phys. Rev. Lett. **64**, 2007 (1990).

[27] N. U. Köylüoğlu, N. Maskara, J. Feldmeier, and M. D. Lukin, Floquet engineering of interactions and entanglement in periodically driven Rydberg chains, arXiv:2408.02741.

[28] J. Feldmeier, N. Maskara, N. U. Köylüoğlu, and M. D. Lukin, Quantum simulation of dynamical gauge theories in periodically driven Rydberg atom arrays, arXiv:2408.02733.

[29] P. Fendley, K. Sengupta, and S. Sachdev, Competing density-wave orders in a one-dimensional hard-boson model, Phys. Rev. B **69**, 075106 (2004).

[30] I. Lesanovsky and H. Katsura, Interacting Fibonacci anyons in a Rydberg gas, Phys. Rev. A **86**, 041601(R) (2012).

[31] A. Hudomal, J.-Y. Desaules, B. Mukherjee, G.-X. Su, J. C. Halimeh, and Z. Papić, Driving quantum many-body scars in the PXP model, Phys. Rev. B **106**, 104302 (2022).

[32] M. D. Lukin, M. Fleischhauer, R. Cote, L. M. Duan, D. Jaksch, J. I. Cirac, and P. Zoller, Dipole blockade and quantum information processing in mesoscopic atomic ensembles, Phys. Rev. Lett. **87**, 037901 (2001).

[33] J.-H. Choi, B. Knuffman, T. C. Liebisch, A. Reinhard, and G. Raithel, Cold Rydberg atoms, Adv. At. Mol. Opt. Phys. **54**, 131 (2007).

[34] M. Weidemüller, There can be only one, Nat. Phys. **5**, 91 (2009).

[35] J. D. Pritchard, D. Maxwell, A. Gauguet, K. J. Weatherill, M. P. A. Jones, and C. S. Adams, Cooperative atom-light interaction in a blockaded Rydberg ensemble, Phys. Rev. Lett. **105**, 193603 (2010).

[36] A. Gaëtan, Y. Miroshnychenko, T. Wilk, A. Chotia, M. Viteau, D. Comparat, P. Pillet, A. Browaeys, and P. Grangier, Observation of collective excitation of two individual atoms in the Rydberg blockade regime, Nat. Phys. **5**, 115 (2009).

[37] D. Barredo, S. Ravets, H. Labuhn, L. Béguin, A. Vernier, F. Nogrette, T. Lahaye, and A. Browaeys, Demonstration of a strong Rydberg blockade in three-atom systems with anisotropic interactions, Phys. Rev. Lett. **112**, 183002 (2014).

[38] F. M. Gambetta, W. Li, F. Schmidt-Kaler, and I. Lesanovsky, Engineering nonbinary Rydberg interactions via phonons in an optical lattice, Phys. Rev. Lett. **124**, 043402 (2020).

[39] V. Bharti, S. Sugawa, M. Kunimi, V. S. Chauhan, T. P. Mahesh, M. Mizoguchi, T. Matsubara, T. Tomita, S. de Léséleuc, and K. Ohmori, Strong spin-motion coupling in the ultrafast dynamics of Rydberg atoms, Phys. Rev. Lett. **133**, 093405 (2024).

[40] M. Magoni, P. Mazza, and I. Lesanovsky, Phonon dressing of a facilitated one-dimensional Rydberg lattice gas, SciPost Phys. Core **5**, 041 (2022).

[41] J. I. Cirac, R. Blatt, P. Zoller, and W. D. Phillips, Laser cooling of trapped ions in a standing wave, Phys. Rev. A **46**, 2668 (1992).

[42] See Supplemental Material at http://link.aps.org/supplemental/10.1103/PhysRevA.111.L041104 for the derivation of $\mathcal{U}(T)$, a discussion about dressing under ultrastrong laser pulses, and the spin-motion echo. Additionally, it discusses decoherence in the adiabatic dressing protocol, the ratio $\mathcal{V}_3/\mathcal{V}_2$, and spin-motion coupling.

[43] T. P. Mahesh, T. Matsubara, Y. T. Chew, T. Tomita, S. de Léséleuc, and K. Ohmori, Generation of 480 nm picosecond pulses for ultrafast excitation of Rydberg atoms, arXiv:2408.02324.

[44] F. M. Gambetta, C. Zhang, M. Hennrich, I. Lesanovsky, and W. Li, Long-range multibody interactions and three-body antiblockade in a trapped Rydberg ion chain, Phys. Rev. Lett. **125**, 133602 (2020).

[45] C. Nill, K. Brandner, B. Olmos, F. Carollo, and I. Lesanovsky, Many-body radiative decay in strongly interacting Rydberg ensembles, Phys. Rev. Lett. **129**, 243202 (2022).

[46] I. I. Ryabtsev, I. I. Beterov, D. B. Tretyakov, V. M. Entin, and E. A. Yakshina, Doppler- and recoil-free laser excitation of Rydberg states via three-photon transitions, Phys. Rev. A **84**, 053409 (2011).

[47] J. Eschner, G. Morigi, F. Schmidt-Kaler, and R. Blatt, Laser cooling of trapped ions, J. Opt. Soc. Am. B **20**, 1003 (2003).

[48] S. Stenholm, The semiclassical theory of laser cooling, Rev. Mod. Phys. **58**, 699 (1986).

[49] K. E. Cahill and R. J. Glauber, Ordered expansions in boson amplitude operators, Phys. Rev. **177**, 1857 (1969).

[50] D. Petrosyan and K. Mølmer, Binding potentials and interaction gates between microwave-dressed Rydberg atoms, Phys. Rev. Lett. **113**, 123003 (2014).

[51] S. Sevinçli and T. Pohl, Microwave control of Rydberg atom interactions, New J. Phys. **16**, 123036 (2014).

[52] P. Scholl, H. J. Williams, G. Bornet, F. Wallner, D. Barredo, L. Henriet, A. Signoles, C. Hainaut, T. Franz, S. Geier, A. Tebben, A. Salzinger, G. Zürn, T. Lahaye, M. Weidemüller, and A. Browaeys, Microwave engineering of programmable XXZ Hamiltonians in arrays of Rydberg atoms, PRX Quantum **3**, 020303 (2022).

[53] M. Kastner, P. Osterholz, and C. Gross, Ancilla-free measurement of out-of-time-ordered correlation functions: General measurement protocol and Rydberg atom implementation, arXiv:2403.08670.

[54] M. H. Goerz, T. Calarco, and C. P. Koch, The quantum speed limit of optimal controlled phasegates for trapped neutral atoms, J. Phys. B: At. Mol. Opt. Phys. **44**, 154011 (2011).

[55] T. Keating, R. L. Cook, A. M. Hankin, Y.-Y. Jau, G. W. Biedermann, and I. H. Deutsch, Robust quantum logic in neutral atoms via adiabatic Rydberg dressing, Phys. Rev. A **91**, 012337 (2015).

[56] A. Mitra, M. J. Martin, G. W. Biedermann, A. M. Marino, P. M. Poggi, and I. H. Deutsch, Robust Mølmer-Sørensen gate for neutral atoms using rapid adiabatic Rydberg dressing, Phys. Rev. A **101**, 030301(R) (2020).

[57] A. Mitra, S. Omanakuttan, M. J. Martin, G. W. Biedermann, and I. H. Deutsch, Neutral-atom entanglement using adiabatic Rydberg dressing, Phys. Rev. A **107**, 062609 (2023).

[58] M. M. Müller, M. Murphy, S. Montangero, T. Calarco, P. Grangier, and A. Browaeys, Implementation of an experimentally feasible controlled-phase gate on two blockaded Rydberg atoms, Phys. Rev. A **89**, 032334 (2014).

[59] F. Robicheaux, T. M. Graham, and M. Saffman, Photon-recoil and laser-focusing limits to Rydberg gate fidelity, Phys. Rev. A **103**, 022424 (2021).

[60] N. Schine, A. W. Young, W. J. Eckner, M. J. Martin, and A. M. Kaufman, Long-lived Bell states in an array of optical clock qubits, Nat. Phys. **18**, 1067 (2022).

[61] S. Trotzky, P. Cheinet, S. Fölling, M. Feld, U. Schnorrberger, A. M. Rey, A. Polkovnikov, E. A. Demler, M. D. Lukin, and I. Bloch, Time-resolved observation and control of superexchange interactions with ultracold atoms in optical lattices, Science **319**, 295 (2008).

[62] Z. Zhang, M. Yuan, B. Sundar, and K. R. A. Hazzard, Motional decoherence in ultracold-Rydberg-atom quantum simulators of spin models, Phys. Rev. A **110**, 053321 (2024).

[63] J. R. Johansson, P. D. Nation, and F. Nori, QuTiP 2: A Python framework for the dynamics of open quantum systems, Comput. Phys. Commun. **184**, 1234 (2013).

[64] L. Béguin, A. Vernier, R. Chicireanu, T. Lahaye, and A. Browaeys, Direct measurement of the van der Waals interaction between two Rydberg atoms, Phys. Rev. Lett. **110**, 263201 (2013).

[65] J. B. Balewski, A. T. Krupp, A. Gaj, S. Hofferberth, R. Löw, and T. Pfau, Rydberg dressing: Understanding of collective many-body effects and implications for experiments, New J. Phys. **16**, 063012 (2014).